Whole-tree chambers for elevated atmospheric CO_2 experimentation and tree-scale flux measurements in south-eastern Australia: the Hawkesbury Forest Experiment

Craig V.M. Barton[a,*], David S. Ellsworth[b], Belinda E. Medlyn[c], Remko A. Duursma[b], David T. Tissue[b], Mark A. Adams[d], Derek Eamus[e], Jann P. Conroy[b], Ross E. McMurtrie[f], Jan Parsby[g], Sune Linder[h]

[a] *Forest Science Centre, Industry and Investment NSW, PO Box 100, Beecroft, NSW 2119 AUSTRALIA*

[b] *Centre for Plants and the Environment, University of Western Sydney, Locked Bag 1797,Penrith South DC, NSW 1797 AUSTRALIA*

[c] *Department of Biological Sciences, Macquarie University, North Ryde, NSW 2109 AUSTRALIA*

[d] *Faculty of Agriculture, Food & Natural Resources, University of Sydney, Sydney, NSW 2006 AUSTRALIA*

[e] *Department of Environmental Sciences, University of Technology Sydney, PO Box 123, Broadway, NSW 2007 AUSTRALIA*

[f] *School of Biological Earth and Environmental Sciences, University of New South Wales, Sydney, NSW 2052 AUSTRALIA*

[g] *Biotronic AB, Konvaljevägen 12 A,SE- 756 51 Uppsala, SWEDEN*

[h] *Southern Swedish Forest Research Centre, Swedish University of Agricultural Sciences,PO Box 49, SE-230 53 Alnarp, SWEDEN*

*Corresponding author: Craig.Barton@industry.nsw.gov.au

Keywords: carbon dioxide assimilation; carbon dioxide enrichment; *Eucalyptus saligna*; Tree photosynthesis;

Abstract (277 words)

Resolving ecophysiological processes in elevated atmospheric CO_2 (C_a) at scales larger than single leaves poses significant challenges. Here, we describe a field-based experimental system designed to grow trees up to 9 m tall in elevated C_a with the capacity to control air temperature and simultaneously measure whole-tree gas exchange. In western Sydney, Australia, we established the Hawkesbury Forest Experiment (HFE) where we built whole-tree chambers (WTC) to measure whole-tree CO_2 and water fluxes of an evergreen broadleaf tree, *Eucalyptus saligna*. A single *E. saligna* tree was grown from seedling to small tree within each of 12 WTCs; six WTCs were maintained at ambient C_a and six WTCs were maintained at elevated C_a, targeted at ambient C_a + 240 μmol mol^{-1}. All 12 WTCs were controlled to track ambient outside air temperature (T_{air}) and air water vapour deficit (D_{air}). During the experimental period, T_{air}, D_{air} and C_a in the WTCs were within 0.5 ºC, 0.3 kPa, and 15 μmol mol^{-1} of the set-points for 90% of the time, respectively. Diurnal responses of whole-tree CO_2 and water vapour fluxes are analysed, demonstrating the ability of the tree chamber system to measure rapid environmental responses of these fluxes of entire trees. The light response of CO_2 uptake for entire trees showed a clear diurnal hysteresis, attributed to stomatal closure at high D_{air}. Tree-scale CO_2 fluxes confirm the hypothesised deleterious effect of chilling night-time temperatures on whole-tree carbon gain in this subtropical *Eucalyptus*. The whole-tree chamber flux data add an invaluable scale to measurements in both ambient and elevated C_a and allow us to elucidate the mechanisms driving tree productivity responses to elevated C_a in interaction with water availability and temperature.

1. Introduction

Atmospheric CO_2 concentration (C_a) has risen from 280 μmol mol^{-1} to the current concentration of *ca*. 390 μmol mol^{-1} over the last 150 years, and continues to rise at a rate of 15 – 20 μmol mol^{-1} per decade (Canadell et al., 2007). Exposure to elevated C_a generally stimulates tree growth (Curtis and Wang, 1998; Norby et al., 1999), increases (20 - 80%) leaf level light-saturated photosynthesis (A_{sat}; reviewed in Ellsworth et al., 2004; Ainsworth and Rogers, 2007), decreases leaf-level stomatal conductance (g_s; Berryman et al., 1994; Medlyn et al., 2001; Ainsworth and Rogers, 2007), and subsequently increases leaf-level water use efficiency (WUE; Field et al., 1995; Wullschleger et al., 2002; Morgan et al., 2004). Although we have excellent techniques for directly measuring gas exchange in single leaves of plants exposed to elevated C_a, few experimental systems resolve gas exchange in elevated C_a at larger scales (Wallin et al., 2001; Dore et al., 2003). Ecophysiological schemes for scaling leaf-level behaviour to larger scales can only approximate CO_2 and water fluxes at the whole-tree level. In order to validate such models, we require a system to measure whole-tree fluxes of CO_2 and water and their response to the environment.

A wide range of experimental systems has been developed to expose plants to elevated C_a, including growth chambers, glasshouses, open-top chambers, field- and laboratory-based mesocosms, and most recently field-based free air CO_2 enrichment (FACE) facilities (*e.g.* Drake et al., 1989; Barton et al., 1993; Whitehead et al., 1995; Griffin et al., 1996; Hendrey et al., 1999). Air temperature may also be controlled in all of these experimental systems except FACE. However, larger trees (>2 - 3 m tall) may only be grown in the field in open-top chambers and FACE, and neither facility is capable of simultaneously exposing trees to elevated C_a and measuring whole-tree fluxes of CO_2 and water. On the other hand, whole-tree chambers (WTC) can precisely maintain elevated C_a and air temperature (T_{air}) for trees up to 9 m tall whilst growing in the field, and can resolve whole-tree CO_2 and water vapour fluxes (Medhurst et al., 2006). In addition, the cost of building and maintaining WTCs is substantially less than that of FACE (Saxe et al., 1998).

Here we describe a unique field-based experimental system designed to grow trees up to 9 m tall in elevated C_a with the capacity to control T_{air} and simultaneously measure whole-tree gas exchange. In western Sydney (Australia), we established the Hawkesbury Forest Experiment (HFE) where we installed WTCs to measure whole-tree CO_2 and water fluxes in an evergreen broadleaf tree, *Eucalyptus saligna* Sm.. A single *E. saligna* tree was grown from seedling to 6.5 m tall within each of 12 WTCs for more than one year. Six WTCs were maintained at ambient CO_2 (C_a tracked outside conditions) and six WTCs were maintained at elevated CO_2 (ambient C_a + 240 µmol mol^{-1}). All 12 WTCs were controlled to track ambient outside T_{air} and air water vapour deficit (D_{air}). Chamber performance characteristics are described in addition to the impact of variation in daily light (Q) and D_{air} on whole-tree fluxes of CO_2 and water.

2. Materials and methods

2.1. Site and experiment description

The Hawkesbury Forest Experiment (HFE) site is situated on an alluvial floodplain near the Hawkesbury River in western Sydney (Australia) at 25 m a.s.l. elevation (33°36’40” S, 150°44’26.5” E). The 5 ha HFE was established in a paddock, which had been converted from native pasture grasses more than a decade earlier. In the HFE, 2000 trees of *E. saligna* and 2000 trees of *E. sideroxylon* were planted at a stocking rate of 1000 trees ha^{-1} (2.6 x 3.85 tree spacing) in April 2007. Soils at the HFE are in the Clarendon Formation (Chromosol; Isbell, 1996), an alluvial formation of low-fertility sandy loam soils (top 70 cm) with low organic matter content (0.7%), moderate to low fertility (available P, 8 mg kg-1; exchangable cations K 0.19; Ca 1.0; Mg 0.28 meq 100g-1) and low water holding capacity. There is a partially cemented hard layer with numerous manganese nodules (70 - 100 cm), and a clay layer (below 100 cm). Permanent ground water is a minimum of 15 m below the soil surface.

The climate in the region where the experiment was conducted is sub-humid temperate. Mean annual temperature at this location is 17 °C, with a mean maximum temperature of the hottest month of 29 °C, and mean minimum temperature of the coldest month of 3 °C. Frost events occur an average of 13 times annually (Australian Bureau of Meteorology; www.bom.gov.au).

The long-term mean annual rainfall is 801 mm, with 1^{st} and 9^{th} deciles for rainfall of 528 and 1075 mm, respectively. The wettest months are typically in the summer (November and February) and the driest months are in the winter (July and August); however, inter-annual variation is very large. The mean ratio of annual precipitation to potential evapotranspiration (FAO-56; Food and Agriculture Organization of the United Nations) is approximately 0.6.

2.2. Whole-Tree Chambers

Twelve whole-tree chambers (WTCs; Fig. 1), previously used in an elevated C_a experiment in a boreal forest in Sweden (Medhurst et al., 2006), were shipped to Australia and installed at the HFE in July 2006. Within each WTC, one 30 cm tall, six month old seedling of *E. saligna* (provenance Styx River, NSW; seedlot 20752 CMA from the Australian Tree Seed Centre, Clayton South, Vic., Australia) was planted in April 2007 and supplied with an initial fertilisation of 50 g of $(NH_4)_2PO_4$ and 10 mm of water every 3^{rd} day to ensure good establishment. Six WTCs were operated to track ambient C_a and six WTCs were operated at elevated C_a (ambient C_a + 240 μmol mol^{-1}), while all 12 WTCs controlled T_{air} to maintain ambient outside conditions. A treatment target C_a of +240 μmol mol^{-1} was chosen to be similar to C_a used in recent free-air CO_2 enrichment experiments, and is anticipated in *ca*. 50 years (Pacala and Sokolow, 2004; IPCC Special Report 2001 at http://www.grida.no/climate/ipcc/emission/). In addition, six control plots were established that were identical to the WTC plots, but without WTCs. Comparision of tree growth and leaf level gas exchange measured on these trees with similar measurements on the ambient chambered trees enables the assessment of any potential chamber effects.

We briefly outline the WTC system and highlight modifications to the WTCs, which were originally designed for relatively cool summers in Sweden (mean maximum temperature of the warmest month of 19 ^{o}C) and required modification to operate under much hotter Australian conditions (> 40 ^{o}C in the summer; mean maximum temperature of the warmest month of 29 ^{o}C). The WTCs are made of a cylindrical aluminum framework 3.25 m in diameter topped with a cone. The WTCs are modular in design and additional cylinders 3.25 x 2.5 m can be installed to increase the internal height from 6.5 m to 9 m (Fig. 1). Each section was initially covered with clear PVC (300 μm thick; Renolit AG, Germany) which transmitted 89% of incident light. The

PVC was replaced in August 2008 with a self-cleaning , ultra-thin Ethylene-Tetrafluroethylene (ETFE) co-polymer film with a high transmission for UV as well as visible light (93 - 94% when new) (F-Clean, AGC Singapore Chemicals Pty. Ltd.). The wall covering extended into the ground and was buried just to the outside of a root barrier, which was composed of heavy duty polyethylene (300 μm thick) that extended to 1 m and into the deeper clay soil. Therefore, the majority of roots and associated CO_2 fluxes in the top 1 m of soil were associated with the single experimental tree planted at the centre of each WTC.

A clear PVC floor (400 μm thick) was installed 45 cm above the ground surface, creating an under-floor volume of *ca.* 4 m^3 (Fig. 1 (A)). The under-floor space was ventilated with a fan blower at the rate of approximately 4 - 8 m^3 per minute, but the space could be sealed to monitor soil CO_2 efflux. Trees were watered regularly during establishment with 10 mm of water every third day. Seven 90° spray nozzles mounted under the floor delivered a uniform coverage of irrigation water to the 10 m^2 of soil surface contained within the underfloor space. Irrigation was under control of the central computer and accurate to $\pm$ 0.1 mm.

The temperature control system consisted of a central refrigeration plant that cooled a glycol/water solution to slightly below (1 - 2 °C) the dew-point temperature of the ambient air. The coolant was delivered to each WTC, where it circulated through a large surface area heat exchanger (2 m x 1 m) mounted in housing on the south side of the WTC. WTC air was continuously circulated through the housing by a frequency controlled fan (Swegon, Kvanum, Sweden) at a rate that could be regulated between 0 and 12,000 m^3 hr^{-1}. Variable baffles regulated by a microprocessor controller in each WTC diverted a portion of the air through the heat exchanger, where it was cooled to the temperature of the coolant before re-entering the WTC (Fig. 1). Excess moisture in the airstream, resulting from transpiration by the tree, was condensed, and then collected and measured using a small tipping bucket pluviometer with a 5 mL resolution (Rain-o-matic, Pronamic, Denmark).

2.3. Chamber CO_2 and water flux measurements

Each WTC was operated as a hybrid between an open-mode and null-balance gas exchange system (Medhurst et al., 2006). Air volume in the WTC was 30 m^3 with a continuous supply of fresh air entering the WTC at a rate of 10 L s^{-1}. A manually adjustable iris orifice allowed adjustment of the flow of air while a digital manometer constantly monitored the pressure drop across the orifice, and thus allowed continuous measurement of the airflow. Pure CO_2 was metered into this air stream to maintain the chamber at its target C_a; hence, the null-balance aspect of whole-tree gas exchange. Air was continuously sampled from each WTC and from a reference line mounted 5 m above the ground, and transported through heated tubing to a manifolded set of 13 three-way solenoid valves, eventually reaching the central infra red gas analyser (IRGA; Licor 7000, Li-Cor Lincoln, Nebraska) in the control cabin. The fast-response time of this IRGA allowed the sampling time period for each WTC to be reduced from 90 s (Medhurst et al., 2006) to 60 s. A full cycle of measurements, including all 12 WTCs and two reference readings, took 14 minutes; whole-tree CO_2 and H_2O fluxes were calculated every cycle.

In addition to a standard meteorological station at the HFE, a separate set of sensors was connected to the WTC central control system including a tipping bucket rain gauge (RG2, Monitor Sensors, QLD, Australia), quantum sensor (LI-190SA, Li-Cor, Inc., USA) and combined air temperature and relative humidity sensor (MP101A, Rotronic Bassersdorf, Switzerland) contained within a ventilated, shielded housing mounted within the tree stand surrounding the WTCs to provide a reference temperature for the WTCs. These sensors were sampled and recorded at one minute intervals.

WTCs were individually instrumented with radiation shielded, ventilated thermistors (10kOhm NTC Accu-Curve, RTI Electronics, Inc, CA, USA), a soil temperature sensor and a soil moisture probe (Theta Probe, Delta T Instruments) at 10 cm depth, a neutron probe access tube installed to 4.75 m, and a PVC access tube installed to 2 m depth to house frequency-domain reflectometer sensors at four depths which were logged every half hour (Sentek EnviroSCAN, Sentek Sensor Technologies, Stepney, S.A., Australia). In addition, two mini-rhizotron tubes were installed at 45° at two distances from the main tree stem in each WTC and used to track root dynamics in the upper 80 cm of soil. See Medhurst et al., 2006 for a complete list of parameters measured and recorded by the system.

2.4 Whole-tree CO_2 and H_2O flux measurements and calculations

The CO_2 flux was calculated from the mass balance of CO_2 entering and leaving the chamber as a result of the chamber ventilation, the pure CO_2 added to maintain the C_a at the target, and any change in storage of CO_2 in the volume of air in the chamber during the measurement cycle.

$$A_{tree} = I + F - V - \Delta S \qquad (1)$$

where A_{tree} is the instantaneous net CO_2 flux from the tree, I is the injection rate of pure CO_2 into the chamber, F is the flow of CO_2 carried into the chamber in the fresh air stream, V is the flow of CO_2 carried out of the chamber as a result of the fresh air entering, and ΔS is the change in storage of CO_2 in the air mass within the chamber volume during the measurement cycle.

The H_2O flux from the tree (E_{tree}) is similarly calculated as the mass balance of water vapour entering and leaving the chamber as a result of the chamber ventilation, taking into account any change in storage of water in the air within the chamber and the amount of water condensed by the cooling system. Calculations for E_{tree} follow those of Medhurst et al. (2006) apart from the following modifications.

We computed the density of fresh air entering the chamber (ρ_{ref}, kg m^{-3}) as

$$r_{ref} = \frac{P_{atm} - H_{ref}}{R \cdot T_{ref}} + \frac{H_{ref}}{R_v \cdot (T_{ref})} \qquad (2)$$

where P_{atm} is the mean atmospheric pressure throughout the measurement cycle (Pa), R the gas constant for dry air (287.05 J K^{-1} kg^{-1}), T_{ref} the mean temperature of the reference air during the measurement cycle (K), H_{ref} (Pa) the water vapour pressure of the reference air during the measurement cycle and R_v the specific gas constant for water vapour (461.495 J kg^{-1} K^{-1}). The volumetric flow of fresh air entering the chamber (F_{in}, L s^{-1}), corrected to standard temperature and pressure was then calculated as

$$F_{in} = \left(k\sqrt{\Delta P \frac{1.2}{r_{ref}}} \right) \frac{273}{T_{ref}} \frac{P_{atm}}{P_{ref}} \quad (3)$$

Where ΔP is the pressure drop across the iris valve in the fresh air delivery tube (Pa), *k* is the flow coefficient for that iris, and P_{ref} standard atmospheric pressure (101.3 kPa). The flow coefficients were checked periodically by measuring temperature, atmospheric pressure and pressure drop across the iris and determining the flow rate of fresh air by measuring the time taken to fill a large lightweight bag (900 L) then inverting equation 3 to find *k*. This parameter was found to be stable over time as long as the iris setting was not changed. To satisfy conservation of mass, the standardised flow of air leaving the chamber (F_{out}, L s^{-1}) was calculated as the standardised flow of air entering the chamber corrected for any change in moisture content according to:

$$F_{out} = F_{in} \frac{P_{atm} - H_{ref}}{P_{atm} - H_{wtc}} \quad (4)$$

where H_{wtc} is the average water vapour pressure of air in the chamber during the measurement cycle (Pa).

We operated the WTCs at a positive pressure of *ca.* 20 Pa in order to minimise gas leaks through gasket-sealed openings (*e.g.* door, emergency ventilation dampers, condensate tube, floor seal around tree trunk, etc.). However, this positive pressure differential may be insufficient to prevent inward diffusion of specific gases (*e.g.* CO_2) when concentration gradients are large. Furthermore, slight errors in the calibration of fresh air-flow, or in mass flow meters used to monitor CO_2 entering the WTC, would lead to errors in the calculation of whole-tree carbon fluxes. In order to assess such errors, the C_a set point was alternated for each WTC every second night. Ambient WTCs were raised to ambient + 240 μmol mol^{-1} and the CO_2 supply was turned off to elevated WTCs from 2100 h to 0400 h. Assuming that respiration is insensitive to short term changes in C_a (Tissue et al., 2002; Gonzales-Meler et al., 2004), any change in the calculated CO_2 flux in response to altering WTC C_a can be attributed to leaks or errors in the calibration of the fresh air flow or CO_2 mass flow sensors. When C_a is changed from elevated to ambient C_a, the supply of CO_2 is instantaneously turned off and WTC C_a gradually declines by dilution from the fresh air entering the WTC. Thus, a sudden step change in apparent respiration rate would indicate an error in calibration of the mass flow sensor, while a gradual change (proportional to the change in C_a between inside and outside the WTC) indicates either incorrect calibration of the fresh air flow or a diffusion leak, which can be mathematically corrected. In the case of a diffusion leak, the correction is by calculation of a leak rate that is proportional to the C_a concentration gradient between the inside and outside of the chamber:

$$P_{corr} = P + ([CO_2]_{WTC} - [CO_2]_{\mathrm{Re}\,f}) \cdot l \qquad (5)$$

where l is the chamber specific leak constant (mol s^{-1}) and $[CO_2]_{WTC}$ and $[CO_2]_{Ref}$ are the chamber and outside reference CO_2 concentrations (μmol mol^{-1}), respectively. Fresh air flows were calibrated on a regular basis and checked, as described above, when an apparent leak/ calibration error was observed.

2.5. Analysis of WTC flux data

A brief analysis of the CO_2 and water flux data is provided to demonstrate the tractability of the measurements and the potential utility of the whole-tree data. The CO_2 fluxes were analysed for two trees growing in ambient C_a over a 160-day period from late February to August 2008, which corresponded to late summer through winter. We analysed responses in terms of the key environmental drivers, which were incident photosynthetically active radiation (400 - 700 nm; Q_{in}), T_{air} and D_{air}.

Based on leaf-level gas exchange data, we expect that canopy CO_2 fluxes should increase and saturate with increasing light levels, but that stomatal closure at high D_{air} reduces the light-saturated CO_2 uptake rates (Eamus et al., 1995; Kirschbaum, 2000). To test these responses, we fitted a non-rectangular hyperbola with a D_{air} modifier function to typical diurnal light responses of chamber CO_2 flux, using SAS PROC NLIN (SAS Institute Inc., Cary, NC, USA.). The non-rectangular hyperbolic equation fitted was as follows:

$$A_C = \frac{a \cdot Q_{in} + A_{C\max} - \sqrt{\left(a \cdot Q_{in} + A_{C\max}\right)^2 - 4 \cdot a \cdot A_{C\max} \cdot Q_{in} \cdot q}}{2 \cdot q} - R_d \qquad (6)$$

where

A_C = net assimilation rate of the crown and whole aboveground portion of the tree, μmol CO_2 m^{-2} ground s^{-1},

Q_{in} = incident photosynthetic photon flux density received by the tree, μmol m^{-2} ground s^{-1},

A_{Cmax} = asymptotic or Q_{in}-saturated net assimilation rate, μmol m^{-2} s^{-1},

α = initial slope of the response curve, which represents the canopy light utilization efficiency

θ = convexity of the response curve (dimensionless, between 0 and 1), and

R_d = dark respiration rate of the aboveground portion of the tree, μmol m^{-2} s^{-1},

The D_{air} modifier function, taken from Lasslop et al. (2010), was as follows:

$$A_{C\max} = \begin{cases} A_{C\max 0} \exp(-k(D_{air} - D_{air0})), D_{air} > D_{air0} \\ A_{C\max 0}, D_{air} \le D_{air0} \end{cases} \qquad (7)$$

where A_{Cmax0} is the maximum assimilation rate in the absence of a limitation by D_{air}, D_{air0} is the threshold vapour pressure deficit at which assimilation begins to be affected by D_{air} and k is the exponent. The WTC data support the use of such a functional relationship where a threshold of about 1 kPa was observed before A_{Cmax} started to reduce in a fairly linear way, which was described well using k=0.25 (data not shown).

3. Results

3.1. Chamber environmental control: C_a, T_{air}, and D_{air}

The WTC C_a control algorithm was modified from Medhurst et al. (2006) to track outside ambient C_a rather than using a constant C_a because of a substantial natural diurnal C_a variation at the HFE: daytime outdoor C_a was *ca*. 380 μmol mol^{-1}, but night-time C_a could be > 500 μmol mol^{-1} depending on wind-speed and time of year. The target C_a was maintained ± 15 μmol mol^{-1} of the target C_a 90% of the time (Fig. 2A-B, and Table 1). The narrow peak of the frequency distribution demonstrated that C_a control tracked the fluctuating ambient C_a well. For the elevated C_a treatment, the WTC was at ambient C_a + 240 μmol mol^{-1}, which produced an average daytime C_a of 620 μmol mol^{-1} and a night-time C_a of 740 μmol mol^{-1} in each WTC. Strict night-time control of C_a in ambient WTCs was not possible because the WTCs do not scrub CO_2 from the atmosphere. Increased C_a at night in all WTCs declined rapidly after sunrise with the onset of photosynthesis.

Despite high radiation loads at high ambient temperatures, we were able to control T_{air} within ± 1 ^{o}C for 90% of the time (Fig. 2C-D) across a range of temperatures from -2.8 to 43.8 ^{o}C (Table 1). T_{air} in the WTCs increased by 1 - 2 ^{o}C relative to ambient air in the few minutes after dawn, when T_{air} was close to dew point. This transient increase was due to the maintenance of coolant liquid at or slightly below dew point. Under such conditions, there was no temperature differential between the heat exchanger and the chamber air. In addition, when extremely dry air (dew point temperature of -1°C) and high T_{air} (35 ^{o}C) conditions occurred, the cooling unit was unable to chill the coolant to the target value. Although a sufficient temperature reduction was maintained to enable regulation of chamber temperatures, WTC humidity was higher than outside air. Under such extreme conditions, D_{air} was ~ 4 kPa in the WTCs while outside D_{air} was ~ 5 kPa; failure to control humidity during these transient and extreme conditions was rare. In general, daytime WTC D_{air} was slightly lower than outside D_{air} (*ca.* 0.2 kPa) as a result of the large transpiration flux, while nighttime WTC D_{air} was occasionally slightly higher than outside D_{air} as a result of the coolant being held 1^{o} C below reference dew point (Fig. 2E-F).

3.2. Leak corrections

We developed leak constants that corrected for small gas diffusion leaks between the WTC and outside air during whole-tree gas exchange measurements. In most cases, the sensitivity of calculated night time flux rates to switching CO_2 control on and off was found to be very small (Fig. 3). There was a slight drift in the uncorrected fluxes when CO_2 injection was turned off and a sudden change when the CO_2 injection was turned on and the C_a concentration gradient between the WTC and outside air was re-established. Leak corrections greatly improved the relationship between night-time respiration and WTC T_{air} (Fig. 4). It should be noted that the impact of these corrections on daytime CO_2 fluxes was generally small (< 5%), but these corrections were very important during transition periods (*e.g.* during dawn and dusk) when trees were near their light compensation point and fluxes were low.

3.3. Chamber gas exchange data

Two ambient WTCs with trees of similar size (basal areas 21 and 23 cm^2; 3-4 m tall) were chosen to illustrate how A_C and E fluxes of whole-trees responded to variation in irradiance and D_{air} on a diurnal basis (Fig. 5). The two representative diurnal courses shown are for mild mid-autumn days. The first day was clear in the morning, but had broken cloud cover in the afternoon, while the second day was clear and sunny all day. The diurnal courses of CO_2 and H_2O fluxes demonstrate the capacity of the WTC system to measure fairly rapid environmental responses of fluxes at the whole-tree scale to fluctuations in light levels. Rainfall occurred during the night preceding the first day shown, explaining why D_{air} remained close to zero until 1100 h. Because of the low D_{air}, H_2O fluxes were very small during that morning. Though watered frequently, the tree crowns were not wetted during outside rain events, so E could still be resolved whilst outside trees were wet. For the two trees, integrated daily carbon uptake was 69 and 54 g d^{-1} on the first day and 82 and 68 g d^{-1} on the second day, respectively. Water loss for the two trees was 17 and 12 L on the first day and 26 and 22 L on the second day.

There is also clear evidence of a strong influence of D_{air} on CO_2 and H_2O fluxes (Fig. 6). On the second, sunny day, there was a strong hysteresis in the response of A_C to Q_{in}, (Fig. 6A and B). Several lines of evidence suggest that this hysteresis can be attributed to stomatal closure in response to rising D_{air}. We fitted the non-rectangular hyperbola with D_{air} modifier (equations 6 and 7) to these data and found a very good fit (Fig. 6A, B). The transpirational flux E also shows a hysteresis in response to D_{air}, with higher rates of transpiration in the morning than in the afternoon (Fig. 6C, D), which is consistent with stomatal closure. Also, the ratio of E to A_C increased linearly with D_{air}, but showed no hysteresis (Fig. 6E, F), indicating a close coupling of transpiration and photosynthesis and therefore stomatal control. Note that there was a rapid rise in the ratio of E to A_C towards evening (Fig. 6E, F). This rise occurred because A_C decreased as Q_{in} decreased towards the compensation point in the early evening, while D_{air} remained fairly high and E continued into the night (Fig. 5B). Night-time E was observed frequently especially early in the evening when D_{air} was still high.

Hysteresis in the light response of A_C was observed on most sunny days. For all days with sufficiently high light levels, we calculated the average CO_2 uptake rates for Q_{in} between 900 and 1100 μmol m^{-2} s^{-1} separately for morning and afternoon data, and average D_{air} corresponding to the same time periods. The difference between morning and afternoon CO_2 uptake rates was strongly related to the difference between morning and afternoon D_{air} (Fig. 7), again supporting the hypothesis that hysteresis is driven by stomatal closure as D_{air} rises. This raises the possibility that stomatal closure is in direct response to rising D_{air} or caused by hydraulic limitations due to low leaf water potential.

We also investigated whether the initial slope of the A_C / Q_{in} relationship varied throughout the season. To obtain daily values of the initial slope, we fitted a linear regression for each day to the relationship between morning CO_2 flux data and Q_{in}, when Q_{in} was < 500 μmol m^{-2} s^{-1}, which is typically the linear portion of the A_C / Q_{in} curve. The initial slope values declined during the study period, with average values of around 0.045 mol C mol^{-1} Q in March, declining to 0.03 mol C mol^{-1} Q in July (Fig. 8A). Although leaf area might influence this relationship, there was little change in leaf area between February and August (data not shown). Therefore, the change in slope may be partially attributed to lower night-time temperatures observed in the winter, as minimum night-time temperature decreases below 4 °C (Fig. 8B).

4. Discussion

In this paper, we describe the operation of a unique experimental facility established in south-eastern Australia to study the response of whole-trees to elevated C_a and interactions with other climate change factors. The experiment uses a sophisticated whole-tree chamber system to measure whole-tree CO_2 and H_2O fluxes in field conditions. The performance of the WTCs is clearly demonstrated by their capacity to maintain C_a, T_{air} and D_{air} close to the desired target levels (Table 1; Fig. 2). Despite being designed for boreal conditions in northern Sweden, climate control by the chambers was excellent even in very hot, dry conditions during the Australian summer, with T_{air} exceeding 35 ºC. Modifications and improvements to the original chamber design reported in Medhurst et al. (2006) have enhanced the ability of the chambers to measure whole-tree fluxes of CO_2 and H_2O at high temporal resolution. The improvements will enable us to collect a valuable dataset to examine whole-tree flux responses to environmental drivers.

Numerous experimental approaches, many of which are complementary, may be used to study the impacts of climate change on plants and ecosystems. For example, the WTC approach is complementary (Fig. 9) to branch bags (Barton et al., 1993), open top chambers (Drake et al., 1989; Ceulemans et al., 1995; Whitehead et al., 1995), growth cabinets and glasshouses (Atwell et al., 2007; Thomas et al., 2007; Ghannoum et al., 2009), mesocosms (Griffin et al., 1996; Tingey et al., 1996) and Free-Air CO_2 Enrichment (FACE) (Hendrey et al., 1999). Nonetheless, few of these other systems allow the measurement of whole-tree fluxes in trees ranging from seedlings to 9 m tall. Measurements of whole-tree fluxes requires enclosing the tree, and although valuable insight into the response of plants to elevated C_a has been obtained using enclosed systems (***e.g.*** Duff et al., 1994), there has been criticism due to the alteration of the microenvironment (Drake et al., 1997; Long et al., 2006). However, greatly improved environmental control in the WTCs was superior to most open-top chambers which relied upon a rapid turnover of fresh air to keep T_{air} and D_{air} close to ambient levels (***e.g***. Leadley, 1993; Whitehead, 1995) whilst sacrificing resolution of gas exchange (Dore et al., 2003). In earlier versions of open-top chambers, T_{air} in the chambers could be 4 - 5 ºC above ambient T_{air} under strong radiant loading (Whitehead et al., 1995), and D_{air} varied depending on environmental conditions and plant size (Piikki et al., 2008). In later designs, Norby et al. (1997) added temperature control to open-top chambers, which improved temperature control ($\pm$ 0.4 ºC), but air was often humidified by the evaporative cooling system. Simultaneous control of both T_{air}

and D_{air} is important as they influence plant physiology and may interact with elevated C_a (Eamus et al., 1995).

In the WTCs, we demonstrated good control of T_{air} and relatively precise control of D_{air} (Fig. 2). Although control was expensive in terms of electricity for the chiller unit, this cost was partly offset by reduced CO_2 consumption through recirculation of air through the heat exchangers and a low rate of fresh air exchange. When air temperatures were > 30 ºC (*ca*. 2.5% of the total time), the main chiller unit had difficulties keeping the coolant below the dew-point of the ambient air because the air-cooled heat exchanger had to remove the heat. Under these conditions, the chamber humidity rose slightly above the target value. However, this was an infrequent problem, restricted to very high vapour pressure deficits (D_{air} > 3 kPa), and unlikely to be of major significance as stomatal closure commenced once the D_{air} was above 1.5 kPa (Barton et al., unpubl.). Modifications to further improve D_{air} control of the WTCs are under consideration.

Open-top chambers and FACE systems are prone to C_a fluctuations due to incursions of parcels of ambient air, especially during windy periods, which can lead to variation in C_a both spatially and temporally (Whitehead et al., 1995; Hendrey et al., 1999; Mikkelsen et al., 2008). In contrast, C_a in the WTCs can be well-regulated both in ambient and elevated treatments, with 1-minute C_a within 3% of the target over 90% of the time (Fig. 3); in comparison, C_a is within 20% of the target 90% of the time for some forest FACE experiments (*e.g*. Duke Forest FACE). The precise control of C_a in the HFE is largely due to the closed nature of the chambers and the fast response time of the CO_2 regulation cycle. While night-time C_a in ambient chambers exceeded the reference concentration (on average by 25 μmol mol^{-1}), due to the slow rate of fresh air exchange and absence of a CO_2 scrubber, the excess CO_2 rapidly disappeared in the morning. Hence, the higher night-time C_a in the ambient chambers is unlikely to have had a significant influence on tree physiology or net carbon exchange.

Apart from control of C_a, D_{air} and T_{air}, chambered systems may also affect the light and wind environment of plants. The chambers were constructed with plastic that transmitted light across a wide frequency without substantially increasing the diffuse light component. However, longwave radiation was altered because the outer canopy leaves were radiatively coupled to the chamber wall, not to the sky. As a result, leaf temperature in the WTC trees was somewhat higher during clear sky nights. This temperature difference was probably small because the longwave radiation balance for a majority of leaves in the canopy was determined by neighbouring leaves rather than the chamber walls. Futhermore, chamber mixing fans maintained air movement within the WTC to minimize leaf boundary layer. This approach kept leaf temperatures in the WTC close to those of outside control trees (data not shown); in the future, we plan to install permanent infrared sensors to monitor canopy temperature.

Due to the large size of the WTCs, it was vital to test for leaks that might have affected measurements of CO_2 and H_2O fluxes. We introduced a new method to test for leaks by reversing the C_a between CO_2 treatments for a few hours at night. We assumed that respiration was insensitive to C_a (Tissue et al., 2002; Gonzales-Meler et al., 2004). This method enabled us to detect leaks or errors in calibration of the CO_2 mass flow and flow of fresh air. Without this test, systematic errors may undermine the validity of the data, especially given small night-time carbon fluxes because of the large concentration gradient between the inside and outside of the chamber. Currently, resolving night-time respiration of trees and ecosystems remains an active area of research (Reichstein et al., 2005; Aubinet 2008; van Gorsel et al., 2009) but subject to a variety of problems in open-air measurement systems that are circumvented in the closed WTCs described here.

One of the main features of the WTCs is the ability to continuously measure whole-tree fluxes of carbon and water in trees grown under controlled environmental conditions. These measurements allow us to study in detail the whole-tree integrated response to environmental variation at high temporal resolution. Previously, only automated shoot cuvette systems yielded similarly high resolution data at the shoot scale (*e.g.* Hari et al., 1999; Kolari et al., 2007) while mesocosms have yielded data from combined plant and soil systems up to 1.5 m tall (Tingey et al., 1996; 2007) . The current WTC experiment differs from the WTC experiment in Sweden with 40-year-old Norway spruce trees (Medhurst et al., 2006) in that *E. saligna* was grown in our experiment under the treatment conditions from seedling until harvest at two years old. This fast-growing *Eucalyptus* species obtained a height of 9 m within two years allowing us to scale water use and carbon uptake of trees of different heights at intervals during their growth.

Models that scale from leaf gas exchange measurements to the tree canopy based on simulation of the within-canopy light gradients can now be tested. These models are widely-used, but typically have only been tested with eddy-covariance data (*e.g.* Amthor et al., 2001; Kramer et al., 2002; Hanson et al., 2005). The main limitation of the eddy-covariance technique is that the measured CO_2 fluxes include autotrophic and heterotrophic respiration, which is often difficult to resolve (Reichstein et al., 2005). The advantage of the WTCs is that their sealed floors allow measurement of net canopy carbon uptake (gross photosynthesis minus aboveground autotrophic respiration). Eddy covariance fluxes are more "noisy" than tree chambers because the measurement area is large (several hectares), often hilly, and variable depending on wind direction and strength. In contrast, the inherent stability of the WTCs over the short term permitted measurements that were markedly less noisy. For example, Lasslop et al. (2010) recently investigated whether the light response of net ecosystem exchange measured by eddy covariance was affected by D_{air}. A marked hysteresis was found, but the hysteresis could be accounted for either by a D_{air} effect on photosynthetic rate or by a strong temperature response of ecosystem respiration. In this experiment fluxes of carbon from the soil are excluded and so the reduction in carbon uptake by the tree canopy as D_{air} increases is most probably the result of stomatal closure. The strength of the limitation was remarkable, particularly because the trees were well-watered throughout the experimental period.

The chamber data also clearly demonstrated the effects of cool night-time temperatures on canopy photosynthesis. Effects of frost on photosynthetic parameters are well known from automated cuvette systems in the boreal zone (*e.g.* Troeng and Linder, 1982; Hari et al., 1999; Kolari et al., 2007), but very limited information exists for temperate evergreen species such as *Eucalyptus*. King and Ball (1998) developed a model of frost effects on leaf photosynthesis based on early studies of frost hardening in snowgum (*E. pauciflora*) (Harwood, 1980, 1981). Their approach has been adopted by process-based models of eucalypt plantation productivity, using empirical parameter tuning to match productivity in cool environments (Sands and Landsberg, 2002; Battaglia et al., 2004). The data presented here will allow us to quantify cold-temperature impacts on *Eucalyptus* photosynthesis at the whole-tree scale for the first time. In conjunction with ancillary leaf-level photosynthesis and chlorophyll fluorescence data, the data will allow us to identify the mechanisms underlying temperature effects on whole-tree CO_2 uptake. These two examples indicate the quality of the whole-tree chamber data and demonstrate their utility in identifying mechanisms of tree response to environmental drivers. This mechanistic information is critical in up-scaling leaf-level measurements and understanding individual tree photosynthesis and transpiration. Whole-tree chamber fluxes can also be compared with whole-system carbon mass-balance (obtained from growth, litterfall, root turnover and soil respiration measurements) and whole-system water balance (obtained from water inputs and soil moisture measurements) to identify and quantify the major mechanisms driving the C_a responses of broadleaved evergreen plantation trees.

Acknowledgements

The project was supported by the Australian Greenhouse Office grant 0506/0085 and subsequently by the Commonwealth Department of Climate Change, with additional funding from the NSW Department of Environment and Climate Change (grant T07/CAG/16). Thanks to Mick Forster, Sigfredo Fuentes for their assistance in maintenance of the experimental site. A special thanks goes to Burhan Amiji whose professionalism, enthusiasm and untiring hard work in maintaining the site has contributed greatly to the success of the project.

References

Ainsworth, E.A., Rogers, A., 2007. The response of photosynthesis and stomatal conductance to rising [CO_2]: mechanisms and environmental interactions. Plant, Cell and Environment 30, 258–270

Amthor, J.S., Chen, J.M., Clein, J.S., Frolking, S E., Goulden, M.L., Grant, R.F., Kimball, J.S., King, A.W., McGuire, A.D., Nikolov, N.T., Potter, C.S., Wang, S., Wofsy, S.C., 2001. Boreal forest CO_2 exchange and evapotranspiration predicted by nine ecosystem process models: Intermodel comparisons and relationships to field measurements. Journal of Geophysical Research - Atmospheres 106, 33623-33648.

Atwell, B.J., Henery, M.L., Rogers, G.S., Seneweera, S.P., Treadwell, M., Conroy, J.P., 2007. Canopy development and hydraulic function in *Eucalyptus tereticornis* grown in drought in CO_2-enriched atmospheres. Functional Plant Biology 34, 1137-1149.

Aubinet M (2008) Eddy covariance CO_2 flux measurements in nocturnal conditions: an analysis of the problem. Ecological Applications, 18, 1368–1378.

Barton, C.V.M., Lee, H.S.J., Jarvis, P.G., 1993. A branch bag and CO_2 control-system for long-term CO_2 enrichment of mature Sitka spruce [*Picea sitchensis* (Bong) Carr]. Plant, Cell and Environment 16, 1139-1148.

Battaglia, M., Sands, P., White, D., Mummery, D., 2004. CABALA: a linked carbon, water and nitrogen model of forest growth for silvicultural decision support. Forest Ecology and Management 193, 251-282.

Berryman, C.A., Eamus, D., Duff, G.A., 1994. Stomatal responses to a range of variables in two tropical tree species grown with CO_2 enrichment. Journal of Experimental Botany 45, 539-546.

Canadell, J.G., Le Quéré, C., Raupach, M.R., Field, C.B., Buitenhuis, E.T., Ciais, P., Conway, T.J., Gillett, N.P., Houghton, R.A., Marland, G., 2007. Contributions to accelerating atmospheric CO_2 growth from economic activity, carbon intensity, and efficiency of natural sinks. Proceedings of the National Academy of the United States of America 104, 18886-18891.

Ceulemans, R., Jiang, X.N., Shao, B.Y., 1995. Effects of elevated atmospheric CO_2 on growth, biomass production and nitrogen allocation of two *Populus* clones. Journal of Biogeography 22, 261-268.

Curtis, P.S., Wang, X.Z., 1998. A meta-analysis of elevated CO_2 effects on woody plant mass, form, and physiology. Oecologia 113, 299-313.

Dore, S., Hymus, G.H., Johnson, D.P., Hinkle, C.R., Valentini, R., Drake, B.G., 2003. Cross validation of open-top chamber and eddy covariance measurements of ecosystem CO_2 exchange in a Florida scrub-oak ecosystem. Global Change Biology 9, 84-95.

Drake, B.G., Leadley, P.W., Arp, W.J., Nassiry, D., Curtis, P.S., 1989. An open top chamber for field studies of elevated atmospheric CO_2 concentration on saltmarsh vegetation. Functional Ecology 3, 363-371.

Drake, B.G., Gonzàlez-Meler M.A., Long, S.P., 1997. More efficient plants: A consequence of rising atmospheric CO_2? Annual Review of Plant Physiology and Plant Molecular Biology 48, 609–639.

Duff, G.A., Berryman, C.A., Eamus, D., 1994. Growth, biomass allocation and foliar nutrient contents of two *Eucalyptus* species of the wet dry tropics of Australia grown under CO_2 enrichment. Functional Ecology 8, 502-508.

Eamus, D., Jarvis, P.G., 1989. The direct effects of increase in the global atmospheric CO_2 concentration on natural and commercial temperate trees and forests. Advances in Ecological Research 19, 1-55.

Eamus, D., Duff, G.A., Berryman, C.A., 1995. Photosynthetic responses to temperature, light flux-density, CO_2 concentration and vapor-pressure deficit in *Eucalyptus tetrodonta* crown under CO_2 enrichment. Environmental Pollution 90, 41-49.

Ellsworth, D.S., Reich, P.B., Naumburg, E.S., Koch, G.W., Kubiske M.E., Smith, S.D., 2004. Photosynthesis, carboxylation and leaf nitrogen responses of 16 species to elevated pCO_2 across four free-air CO_2 enrichment experiments in forest, grassland and desert. Global Change Biology 10, 2121-2138.

Field, C.B., Jackson, R.B., Mooney, H.A., 1995. Stomatal responses to increased CO_2 - Implications from the plant to the global-scale. Plant, Cell and Environment 18, 1214-1225.

Ghannoum, O., Phillips, N.G., Conroy, J.P., Smith, R.A., Attard, R.D., Woodfield, R., Logan, B.A., Lewis, J.D., Tissue, D.T., 2009. Exposure to preindustrial, current and future atmospheric CO_2 and temperature differentially affects growth and photosynthesis in Eucalyptus. Global Change Biology doi: 10.1111/j.1365-2486.2009.02003.x

Gonzalez-Meler, M.A., Taneva, L., Trueman, R.J., 2004. Plant respiration and elevated atmospheric CO_2 concentration: Cellular responses and global significance. Annals of Botany 94, 647-656.

Griffin, K.L., Ross, P.D., Sims, D.A., Luo, Y., Seemann, J.R., Fox, C.A., Ball, J.T., 1996. EcoCELLs: Tools for mesocosm scale measurements of gas exchange. Plant, Cell and Environment 19, 1210-1221.

van Gorsel, E., Delpierre, N., Leuning, R., Black, A., Munger, J. W., Wofsy, S., Aubinet, M., Feigenwinter, C., Beringer, J., Bonal, D., Chen, B. Z., Chen, J. Q., Clement, R., Davis, K. J., Desai, A. R., Dragoni, D., Etzold, S., Grunwald, T., Gu, L. H., Heinesch, B., Hutyra, L. R., Jans, W. W. P., Kutsch, W., Law, B. E., Leclerc, M. Y., Mammarella, I., Montagnani, L., Noormets, A., Rebmann, C., Wharton, S. 2009. Estimating nocturnal ecosystem respiration from the vertical turbulent flux and change in storage of CO_2. Agricultural and Forest Meteorology 149**,** 1919-1930.

Hanson, P.J., Wullschleger, S.D., Norby, R.J., Tschaplinski, T.J., Gunderson, C.A., 2005. Importance of changing CO_2, temperature, precipitation, and ozone on carbon and water cycles of an upland-oak forest: incorporating experimental results into model simulations. Global Change Biology 11, 1402-1423.

Hari, P., Mäkelä, A., Berninger, F., Pohja, T., 1999. Field evidence for the optimality hypothesis of gas exchange in plants. Australian Journal of Plant Physiology 26, 239-244.

Harwood, C.E., 1980. Frost-resistance of subalpine *Eucalyptus* species. 1. Experiments using a radiation frost room. Australian Journal of Botany 28, 587-599.

Harwood, C.E., 1981. Frost-resistance of subalpine *Eucalyptus* species. 2. Experiments using the resistance index method of damage assessment. Australian Journal of Botany 29, 209-218.

Hendrey, G.R., Ellsworth, D.S., Lewin, K.F., Nagy, J., 1999. A free-air enrichment system for exposing tall forest vegetation to elevated atmospheric CO_2. Global Change Biology 5, 293-309.

IPCC., 2001. Special Report on Emissions Scenarios. Published to web by GRID-Arendal at http://www.grida.no/climate/ipcc/emission/

Isbell, R.F., 1996. The Australian Soil Classification. CSIRO Publishing, Australia.

King, D.A., Ball, M.C., 1998. A model of frost impacts on seasonal photosynthesis of *Eucalyptus pauciflora*. Australian Journal of Plant Physiology 25, 27-37.

Kirschbaum, M.U.F., 2000. Forest growth and species distribution in a changing climate. Tree Physiology 20, 309-322.

Kolari, P., Lappalainen, H.K., Hänninen, H., Hari, P., 2007. Relationship between temperature and the seasonal course of photosynthesis in Scots pine at northern timberline and in southern boreal zone. Tellus Series B - Chemical and Physical Meteorology 59, 542-552.

Kramer, K., Leinonen, I., Bartelink, H.H., Berbigier, P., Borghetti, M., Bernhofer, C., Cienciala, E., Dolman, A.J., Froer, O., Gracia, C.A., Granier, A., Grünwald, T., Hari, P., Jans, W., Kellomäki, S., Loustau, D., Magnani, F., Markkanen, T., Matteucci, G., Mohren, G.M.J., Moors, E., Nissinen, A., Peltola, H., Sabate, S., Sanchez, A., Sontag, M., Valentini, R., Vesala, T., 2002. Evaluation of six process-based forest growth models using eddy-covariance measurements of CO_2 and H_2O fluxes at six forest sites in Europe. Global Change Biology 8, 213-230.

Lasslop, G., Reichstein, M., Papale, D., Richardson, A.D., Arneth, A., Barr, A., Stoy, P., Wohlfahrt, G., 2010. Separation of net ecosystem exchange into assimilation and respiration using a light response curve approach: critical issues and global evaluation. Global Change Biology, doi: 10.1111/j.1365-2486.2009.02041.x

Leadley, P.W., Drake, B.G., 1993. Open top chambers for exposing plant canopies to elevated CO_2 concentration and for measuring net gas-exchange. Vegetatio 104, 3-15.

Long, S.P., Ainsworth, E.A., Leakey, A.D.B., Nosberger, J., Ort, D.R., 2006. Food for thought: Lower-than-expected crop yield stimulation with rising CO_2 concentrations. Science 312, 1918-1921.

Medhurst, J., Parsby, J., Linder, S., Wallin, G., Ceschia, E., Slaney, M., 2006. A whole-tree chamber system for examining tree-level physiological responses of field grown trees to environmental variation and climate change. Plant, Cell and Environment 29, 1853-1869.

Medlyn, B.E., Barton, C.V.M., Broadmeadow, M.S.J., Ceulemans, R., De Angelis, P., Forstreuter, M., Freeman, M., Jackson, S. B., Kellomäki, S., Laitat, E., Rey, A., Roberntz, P., Sigurdsson, B.D., Strassemeyer, J., Wang, K., Curtis, P. S., Jarvis, P.G., 2001. Stomatal conductance of forest species after long-term exposure to elevated CO_2 concentration: a synthesis. New Phytologist 149, 247-264.

Mikkelsen, T.N., Beier, C., Jonasson, S., Holmstrup, M., Schmidt, I.K., Ambus, P., Pilegaard, K., Michelsen, A., Albert, K., Andresen, L.C., Arndal, M.F., Bruun, N., Christensen, S., Danbaek, S., Gundersen, P., Jörgensen, P., Linden, L. G., Kongstad, J., Maraldo, K., Prieme, A., Riis-Nielsen, T., Ro-Poulsen, H., Stevnbak, K., Selsted, M.B., Sörensen, P., Larsen, K.S., Carter, M.S., Ibrom, A., Martinussen, T., Miglietta, F., Sverdrup, H., 2008. Experimental design of multifactor climate change experiments with elevated CO2, warming and drought: the CLIMAITE project. Functional Ecology 22, 185-195.

Morgan, J.A., Pataki, D.E., Körner, C., Clark, H., Del Grosso, S.J., Grünzweig, J.M., Knapp, A.K., Mosier, A.R., Newton, P.C.D., Niklaus, P.A., Nippert, J.B., Nowak, R.S., Parton, W.J., Polley, H.W., Shaw, M.R., 2004. Water relations in grassland and desert ecosystems exposed to elevated atmospheric CO_2. Oecologia 140, 11-25.

Norby, R.J., Edwards, N.T., Riggs, J.S., Abner, C.H., Wullschleger, S.D., Gunderson, C.A., 1997. Temperature-controlled open-top chambers for global change research. Global Change Biology 3, 259-267.

Norby, R.J., Wullschleger, S.D., Gunderson, C.A., Johnson, D.W., Ceulemans, R., 1999. Tree responses to rising CO_2 in field experiments: implications for the future forest. Plant, Cell and Environment 22, 683-714.

Pacala, S., Sokolow, R., 2004. Stabilization wedges: Solving the climate problem for the next 50 years with current technologies. Science 305, 968-972.

Piikki, K., De Temmerman, L., Hogy, P., Pleijel, H., 2008. The open-top chamber impact on vapour pressure deficit and its consequences for stomatal ozone uptake. Atmospheric Environment 42, 6513-6522.

Reichstein, M., Falge, E., Baldocchi, D., Papale, D., Aubinet, M., Berbigier, P., Bernhofer, C., Buchmann, N., Gilmanov, T., Granier, A., Grünwald, T., Havrankova, K., Ilvesniemi, H., Janous, D., Knohl, A., Laurila, T., Lohila, A., Loustau, D., Matteucci, G., Meyers, T., Miglietta, F., Ourcival, J. M., Pumpanen, J., Rambal, S., Rotenberg, E., Sanz, M., Tenhunen, J., Seufert, G., Vaccari, F., Vesala, T., Yakir, D., Valentini, R., 2005. On the separation of net ecosystem exchange into assimilation and ecosystem respiration: review and improved algorithm. Global Change Biology 11, 1424-1439.

Sands, P.J., Landsberg, J.J., 2002. Parameterisation of 3-PG for plantation grown *Eucalyptus globulus.* Forest Ecology and Management 163, 273-292.

Saxe, H., Ellsworth, D.S., Heath, J., 1998. Tree and forest functioning in an enriched CO_2 atmosphere. New Phytologist 139, 395-436.

Thomas, D.S., Montagu, K.D., Conroy, J.P., 2007. Temperature effects on wood anatomy, wood density, photosynthesis and biomass partitioning of *Eucalyptus grandis* seedlings. Tree Physiology 27, 251-260.

Tingey, D. T., McVeety, B. D., Waschmann, R., Johnson, M. G., Phillips, D. L., Rygiewicz, P. T., Olszyk, D. M. 1996. A versatile sun-lit controlled-environment facility for studying plant and soil processes. Journal of Environmental Quality 25, 614-625.

Tingey, D. T., Phillips, D. L., Lee, E. H., Waschmann, R. S., Olszyk, D. A., Rygiewicz, P. T. and Johnson, M. G. (2007). Elevated temperature, soil moisture and seasonality but not CO_2 affect canopy assimilation and system respiration in seedling Douglas-fir ecosystems. Agricultural and Forest Meteorology 143, 30-48.

Tissue, D.T., Lewis, J.D., Wullschleger, S.D., Amthor, J.S., Griffin, K.L., Anderson, O.R. 2002. Leaf respiration at different canopy positions in sweetgum (*Liquidambar styraciflua*) grown in ambient and elevated concentrations of carbon dioxide in the field. Tree Physiology 22, 1157-1166.

Troeng, E., Linder, S., 1982. Gas exchange in a 20-year-old stand of Scots pine. I. Net photosynthesis of current and one-year-old shoots within and between seasons. Physiologia Plantarum 54, 7-14.

Wallin, G., Linder, S., Lindroth, A., Räntfors, M., Flemberg, S., Grelle, A., 2001. Carbon dioxide exchange in Norway spruce at the shoot, tree and ecosystem scale. Tree Physiology 21, 969-976.

Whitehead, D., Hogan, K.P., Rogers, G.N.D., Byers, J.N., Hunt, J.E., McSeveny, T.M., Hollinger, D.Y., Dungan, R.J., Earl, W.B., Bourke, M.P., 1995. Performance of large open-top chambers for long-term field investigations of tree response to elevated carbon dioxide concentration. Journal of Biogeography 22, 307-313.

Wullschleger, S.D., Tschaplinski, T.J., Norby, R.J., 2002. Plant water relations at elevated CO_2 - implications for water-limited environments. Plant, Cell and Environment 25, 319-331.

FIGURE CAPTIONS

Fig. 1. Schematic diagram of a whole-tree chamber modified from Medhurst et al. (2006) to highlight new or modified components. The modular chamber consisted of three main components (A, B-D, and E): the chamber base (soil compartment), the tree chamber (aboveground compartment) and a cooling unit placed directly outside the chamber. The diameter of the WTC was 3.25 m. The chamber base (A) was approximately 0.45 m high. The tree chamber consisted of a bottom (B) and top (D) section with a height of 2.5 m and 3.0 m, respectively. An extra section (C), with a height of 2.65 m was added as the trees grew. Major components of the system are indicated in the diagram with numbers: (1) pipe for circulating the chamber air through the cooling unit; a cooling unit (E) consisting of: (2) frequency-controlled fan (0 - 12 000 m^3 h^{-1}); (3) dampers to regulate the amount of air going through the cooling unit; (4) large-surface area heat exchanger; (5) circulating a glycol/water solution maintained at ambient dew point temperature; and (6) fresh air inlet; (7) fan for fresh air; (8) iris damper for flow control of fresh air intake; (9) safety fan connected to a diesel generator, which starts in case of power failure; and (10) a 12-V controlled safety damper working in parallel with a similar damper at the top of the WTC; (11) root barrier to depth of 1 m.

Fig. 2. Frequency of deviations from target values for air temperature (A; T_{air}), chamber CO_2 concentration (B; C_a) and air vapour pressure deficit (C; D_{air}) for ambient and elevated chambers during daytime and night-time for the period 20th February (summer) to 6th August (winter).

Fig. 3. Leak corrections for an elevated C_a chamber over the course of five days and nights. (A) reference and chamber C_a on three nights when CO_2 supply was turned off for a several hours. #

indicates the commencement of CO_2 injection into the chambers and $\$$ the cessation of CO_2 injection; (B) air temperature in the chamber; and, (C) uncorrected and corrected flux of CO_2.

Fig. 4. Uncorrected (A) and corrected night-time CO_2 fluxes (B) plotted against chamber temperature for an elevated chamber during the five successive nights shown in Fig. 3. Closed symbols are data when the CO_2 supply was turned off, and open symbols show when CO_2 supply was on. Values in panel A exceeding zero erroneously suggest a positive CO_2 flux into the plant at night at the coolest temperatures prior to applying the appropriate corrections (eq. 5).

Fig. 5. Diurnal course CO_2 flux (A) (μmol m^{-2} ground s^{-1}) and H_2O flux (B) (mmol m^{-2} ground s^{-1}) over two consecutive days representing contrasting conditions. Photosynthetically active photon flux density (Q; panel C) and vapour pressure deficit of chamber air (D_{air}; panel D) are shown. Grey shading indicates the night period.

Fig. 6. Carbon and water fluxes for two ambient trees on 30th March (autumn). Whole-tree net CO_2 assimilation per unit ground area *versus* photosynthetically active photon flux density (Q_{in}, μmol m^{-2} s^{-1}) is shown with fitted values using the function in Eq. 6 and 7 shown as joined line (A and B). H_2O flux per unit ground area as a function of D_{air} (C and D). Ratio of H_2O flux to CO_2 flux as a transpiration efficiency, plotted against D_{air} (E and F). Data prior to noon are shown with solid circles and after noon as open circles. Note the sudden departure from the strong linear relationship at low light levels early in the morning and late in the afternoon as CO_2 flux diminishes to zero while H_2O flux remains at low levels.

Fig. 7. Difference between whole-tree maximum assimilation rate in the afternoon (A_{1000pm}) and the morning (A_{1000am}), both measured when PPFD was between 900 and 1100 µmol m^{-2} s^{-1}, as a function of the difference in D_{air} measured at the same times.

Fig. 8. Initial slope of the relationship between whole-tree assimilation and incident quantum flux of light (µmol CO_2 / µmol quanta of PAR) for two chambers between February (summer) and August 2008 (winter) as a function of time (A) and minimum temperature of the night preceding the measurement (B) and the minimum daily temperature on each day (C). The line in (A) is the Loess fit, while the lines in (B) are hand-drawn to indicate the general trends in the data and a breakpoint at 4^{o}C.

Fig. 9. Schematic diagram indicating applicability of different ecophysiological techniques for experimental treatments and measurements at a variety of scales. FACE denotes free-air CO_2 enrichment.

Table 1 Absolute deviations of environmental conditions within chambers (C_a, T_{air} and D_{air}) from target values based on outside ambient air conditions during the period 20.02.2008 to 06.08.2008. Mean, median, and 5th and 95th percentiles are shown.

			Mean	Median	5%	95%
C_a deviation (µmol mol^{-1})	Ambient	Day	1.0	0.0	-15.9	21.5
		Night	36.7	25.8	4.9	111.2
	Elevated	Day	1.2	0.1	-9.5	9.6
		Night	-1.7	-0.9	-12.5	6.7
T_{air} deviation (ºC)	Ambient	Day	0.11	0	-0.5	1.3
		Night	-0.18	0	-1.5	0.6
	Elevated	Day	0.12	0	-0.6	1.4
		Night	-0.01	0	-1.1	0.9
D_{air} deviation (kPa)	Ambient	Day	-0.18	-0.15	-0.50	0.11
		Night	-0.02	0.02	-0.30	0.14
	Elevated	Day	-0.07	-0.05	-0.34	0.16
		Night	0.04	0.05	-0.16	0.17

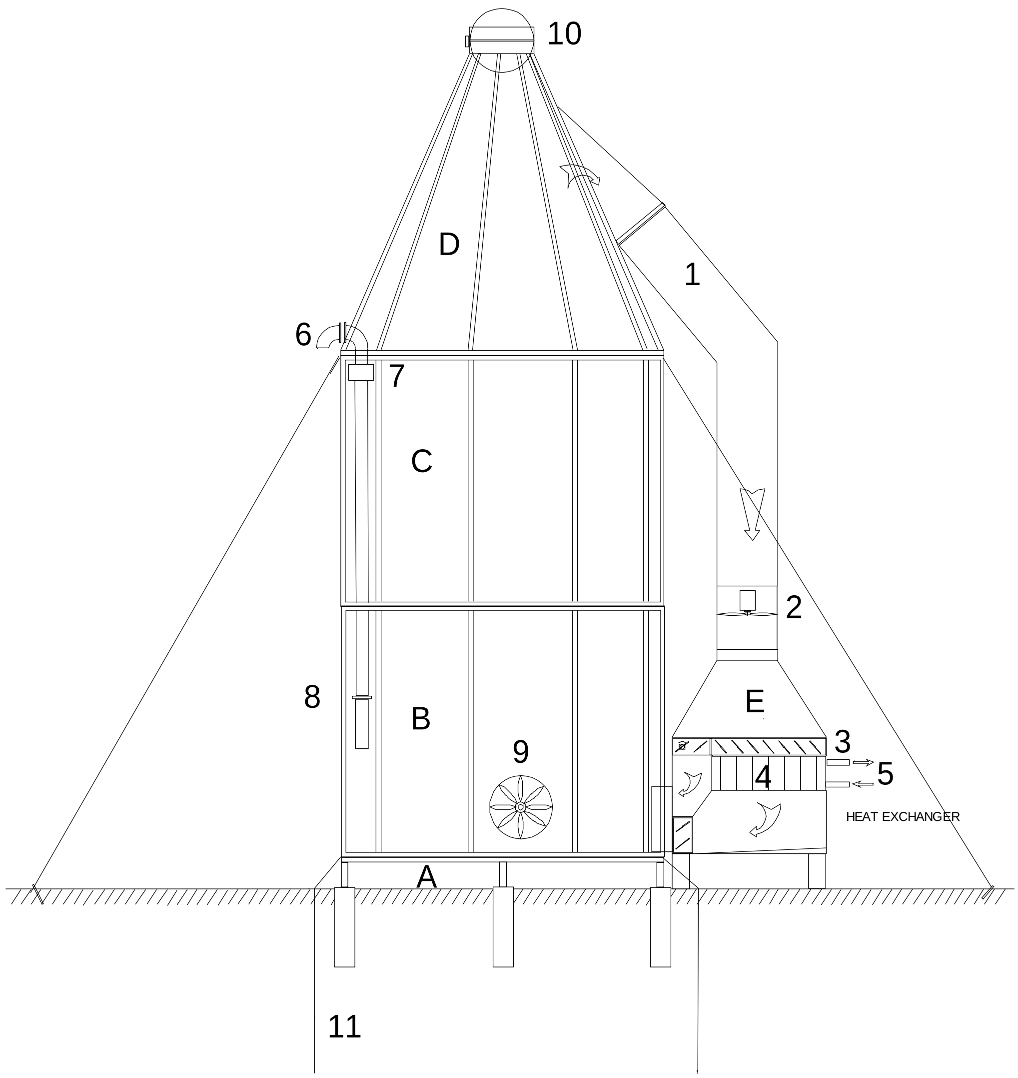

Fig. 1.

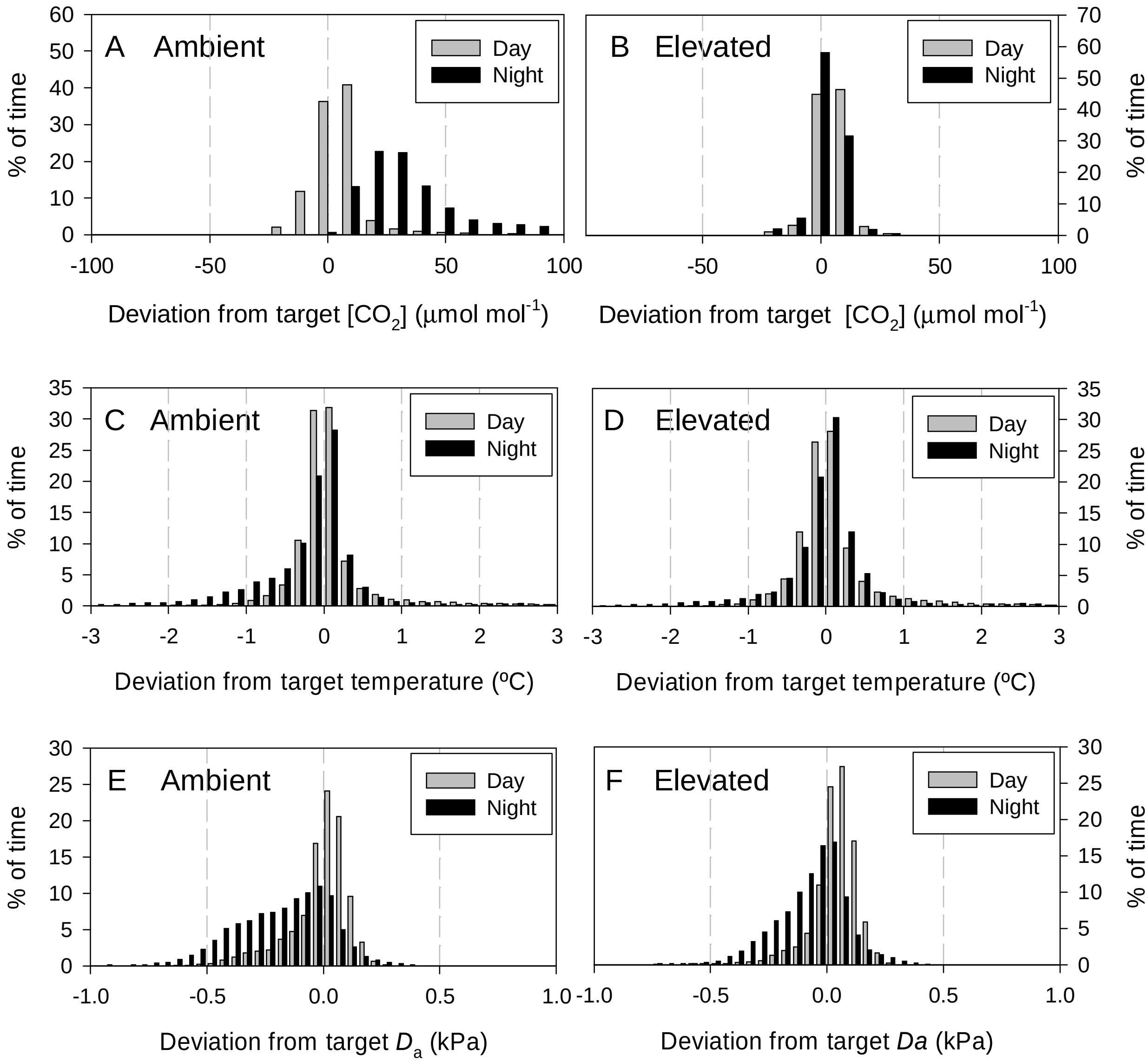
A Ambient
B Elevated
C Ambient
D Elevated
E Ambient
F Elevated
Day
Night
% of time
Deviation from target [CO2] (µmol mol-1)
Deviation from target temperature (ºC)
Deviation from target Da (kPa)
Deviation from target Da (kPa)

Fig. 2.

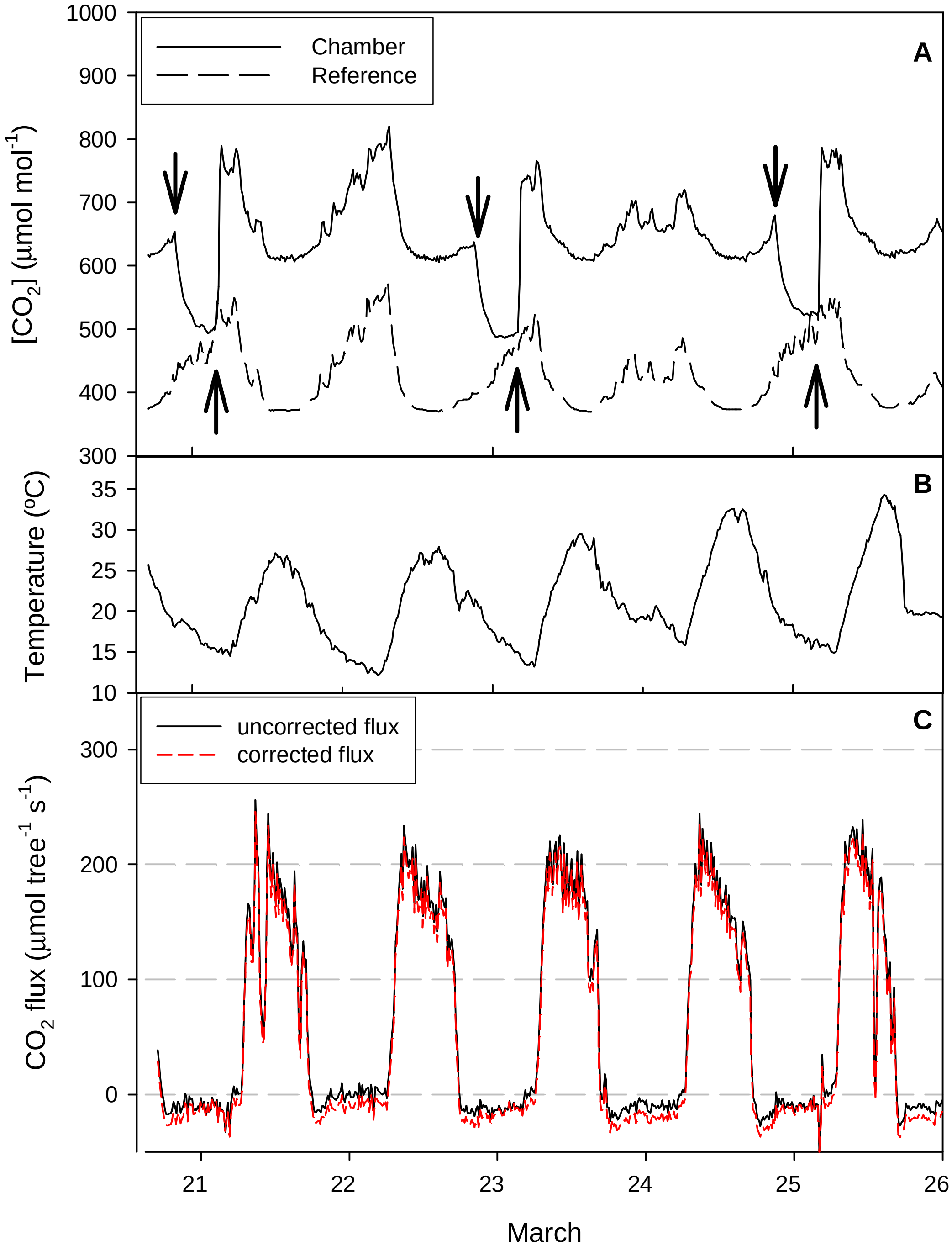
A
Chamber
Reference
[CO2] (µmol mol-1)
1000
900
800
700
600
500
400
300
B
Temperature (ºC)
35
30
25
20
15
10
C
uncorrected flux
corrected flux
CO2 flux (µmol tree-1 s-1)
300
200
100
0
21
22
23
24
25
26
March

Fig. 3.

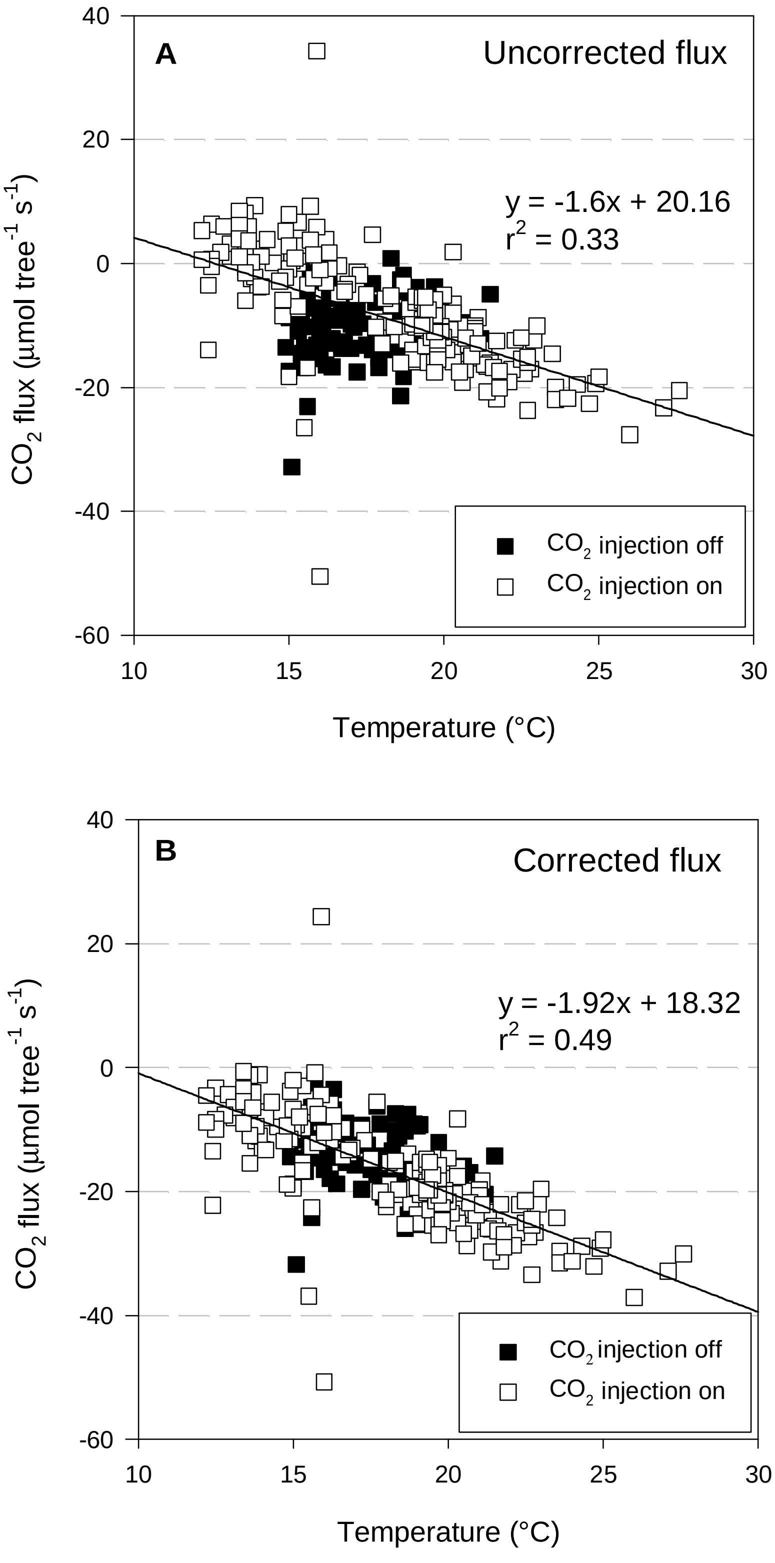
A
Uncorrected flux
y = -1.6x + 20.16
r2 = 0.33
CO2 injection off
CO2 injection on
CO2 flux (µmol tree-1 s-1)
Temperature (°C)
B
Corrected flux
y = -1.92x + 18.32
r2 = 0.49
CO2 injection off
CO2 injection on
CO2 flux (µmol tree-1 s-1)
Temperature (°C)

Fig. 4.

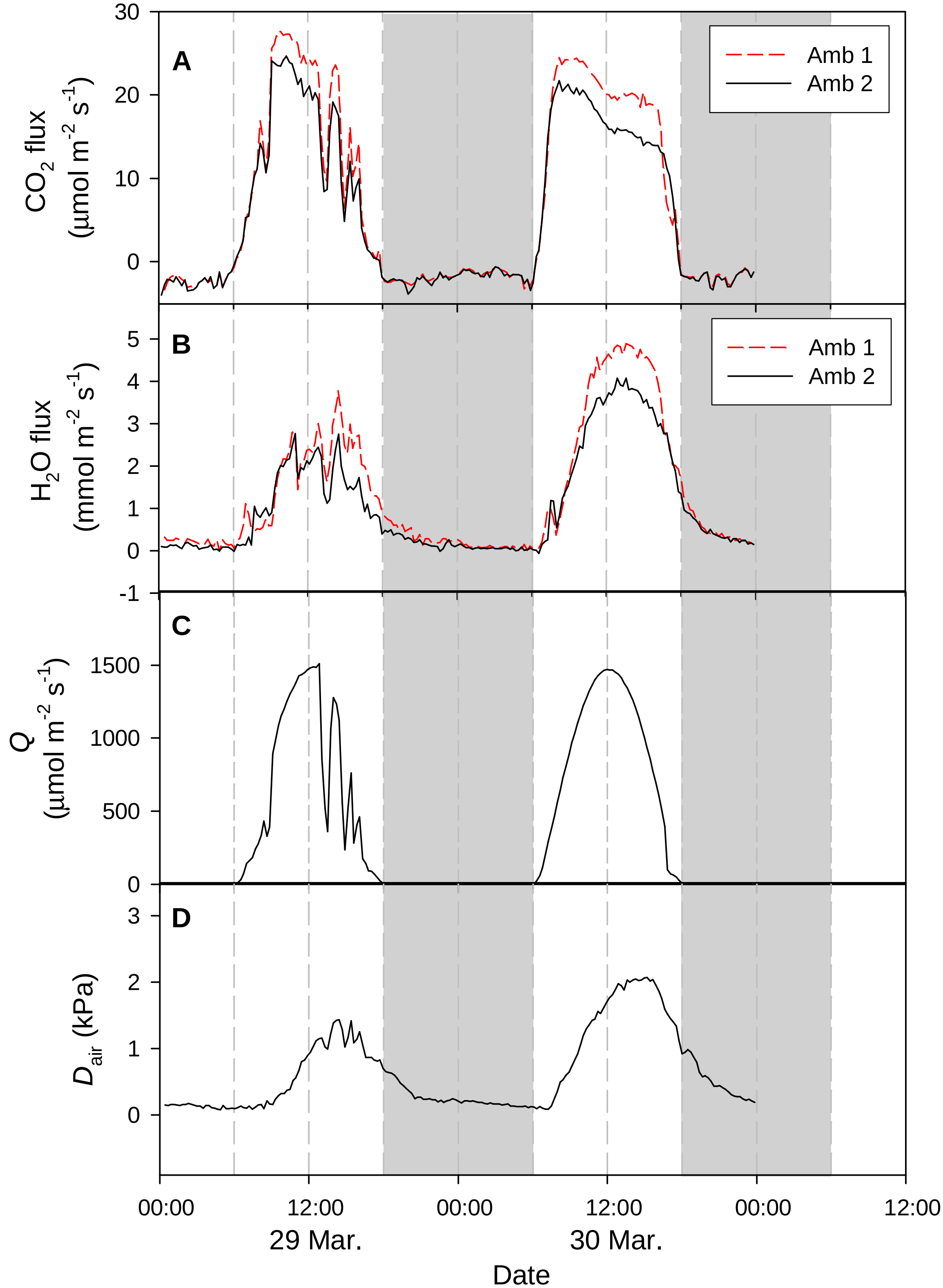

A
B
C
D
Amb 1
Amb 2
CO_2 flux (µmol m-2 s-1)
H_2O flux (mmol m-2 s-1)
Q (µmol m-2 s-1)
D_{air} (kPa)
30
20
10
0
5
4
3
2
1
0
-1
1500
1000
500
0
3
2
1
0
00:00
12:00
00:00
12:00
00:00
12:00
29 Mar.
30 Mar.
Date

1
2 **Fig. 5.**

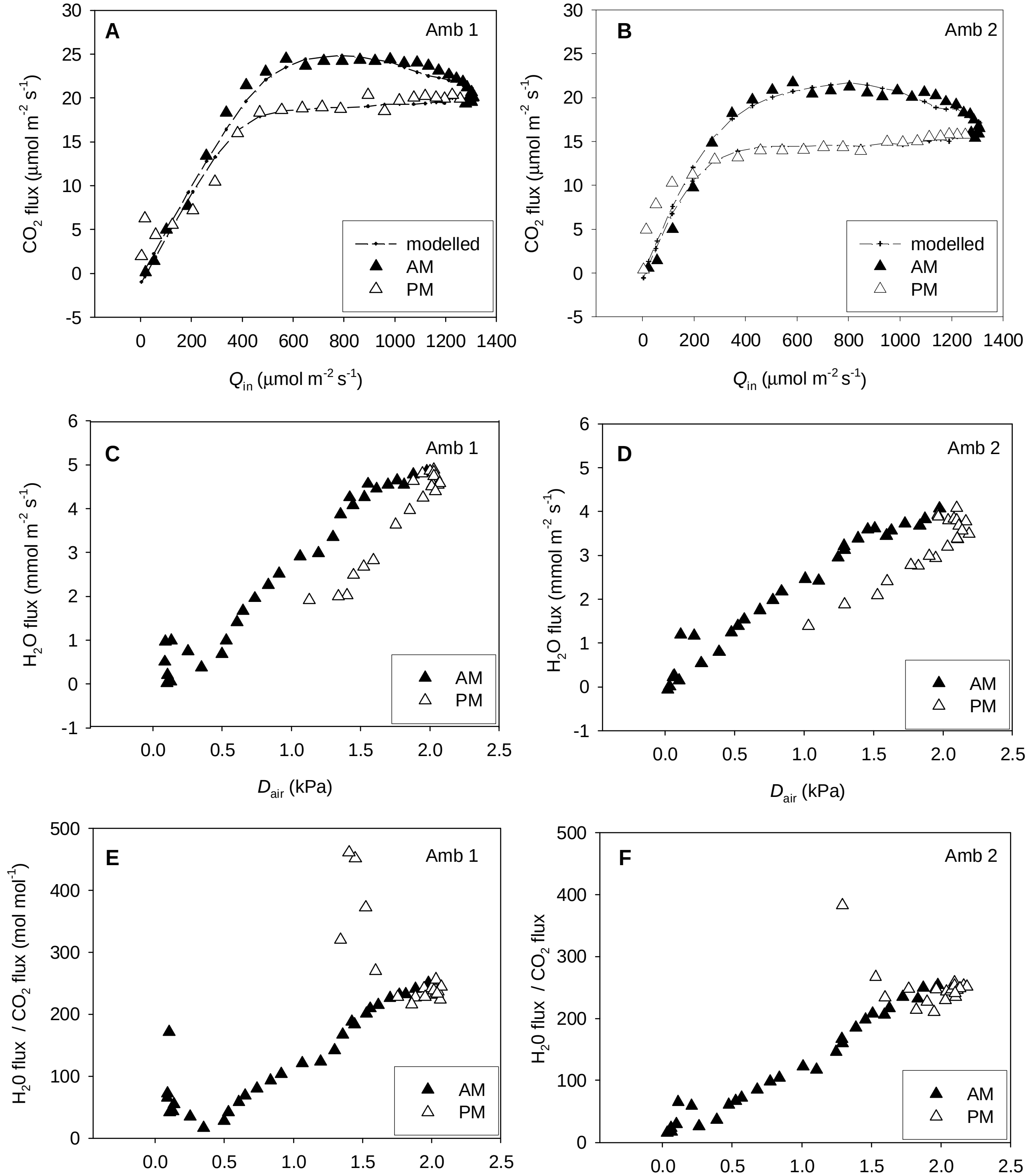
A
Amb 1
B
Amb 2
CO2 flux (µmol m-2 s-1)
Qin (µmol m-2 s-1)
modelled
AM
PM
C
D
H2O flux (mmol m-2 s-1)
Dair (kPa)
E
F
H20 flux / CO2 flux (mol mol-1)
H20 flux / CO2 flux

Fig. 6.

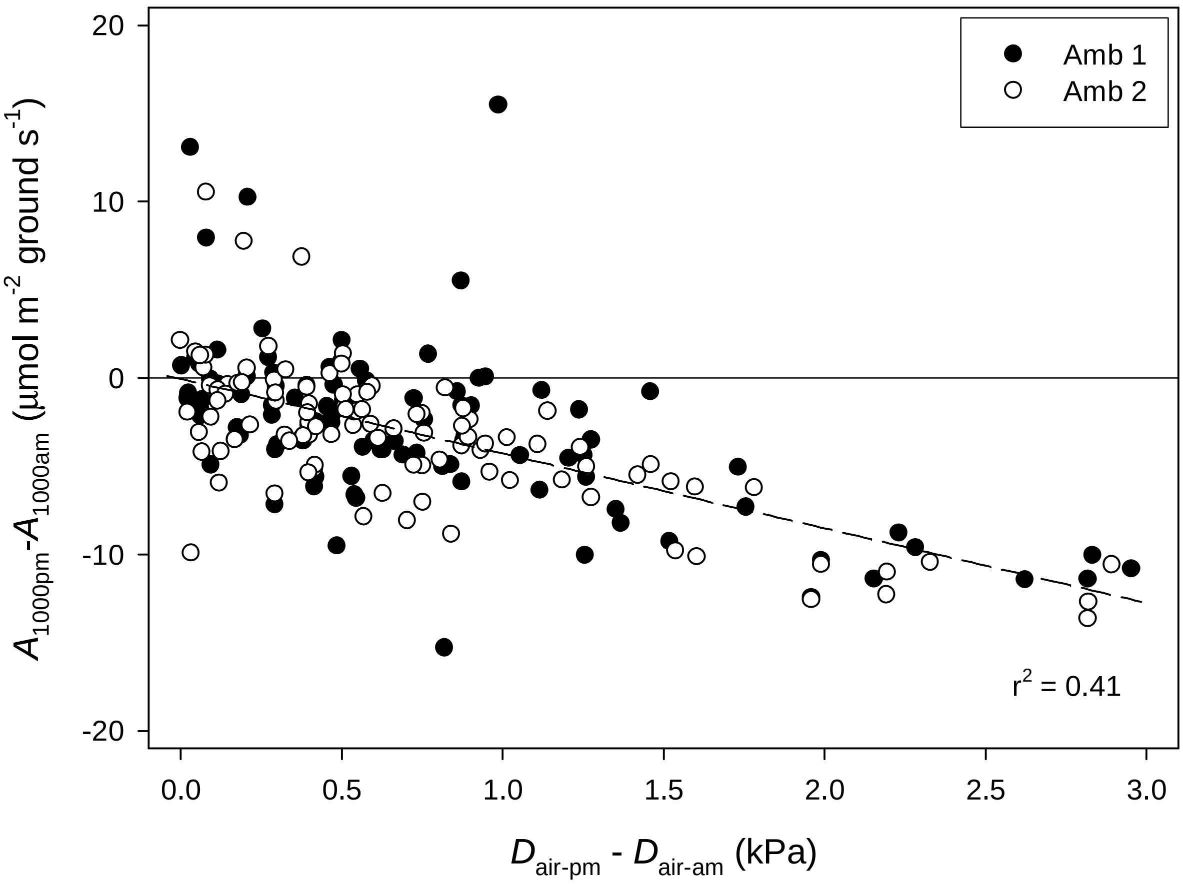
Amb 1
Amb 2
r2 = 0.41
A1000pm-A1000am (µmol m-2 ground s-1)
Dair-pm - Dair-am (kPa)
20
10
0
-10
-20
0.0
0.5
1.0
1.5
2.0
2.5
3.0

Fig. 7.

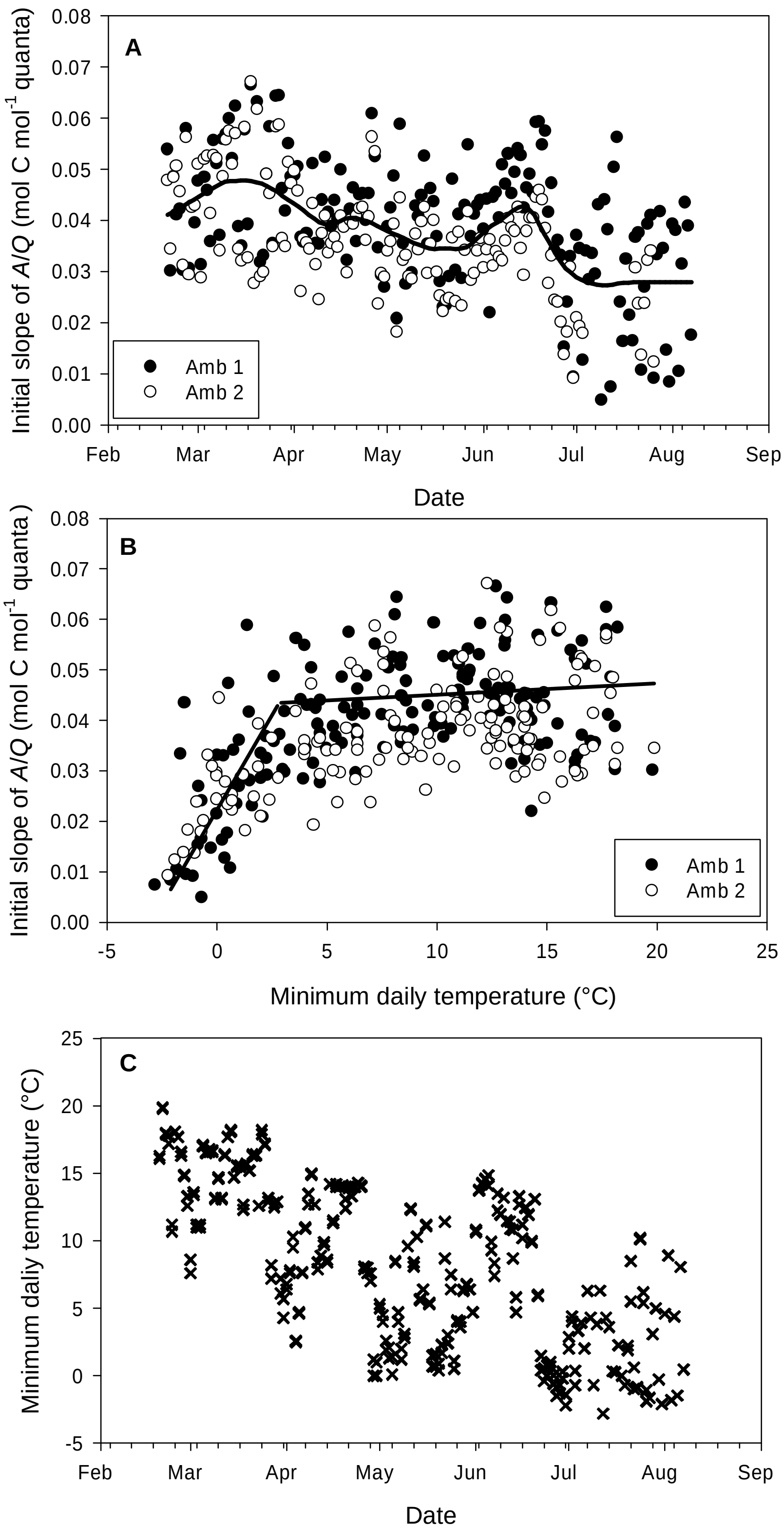
A
B
C
Amb 1
Amb 2
Initial slope of A/Q (mol C mol-1 quanta)
Date
Minimum daily temperature (°C)
Minimum daily temperature (°C)
Feb
Mar
Apr
May
Jun
Jul
Aug
Sep
0.00
0.01
0.02
0.03
0.04
0.05
0.06
0.07
0.08
-5
0
5
10
15
20
25

Fig. 8.

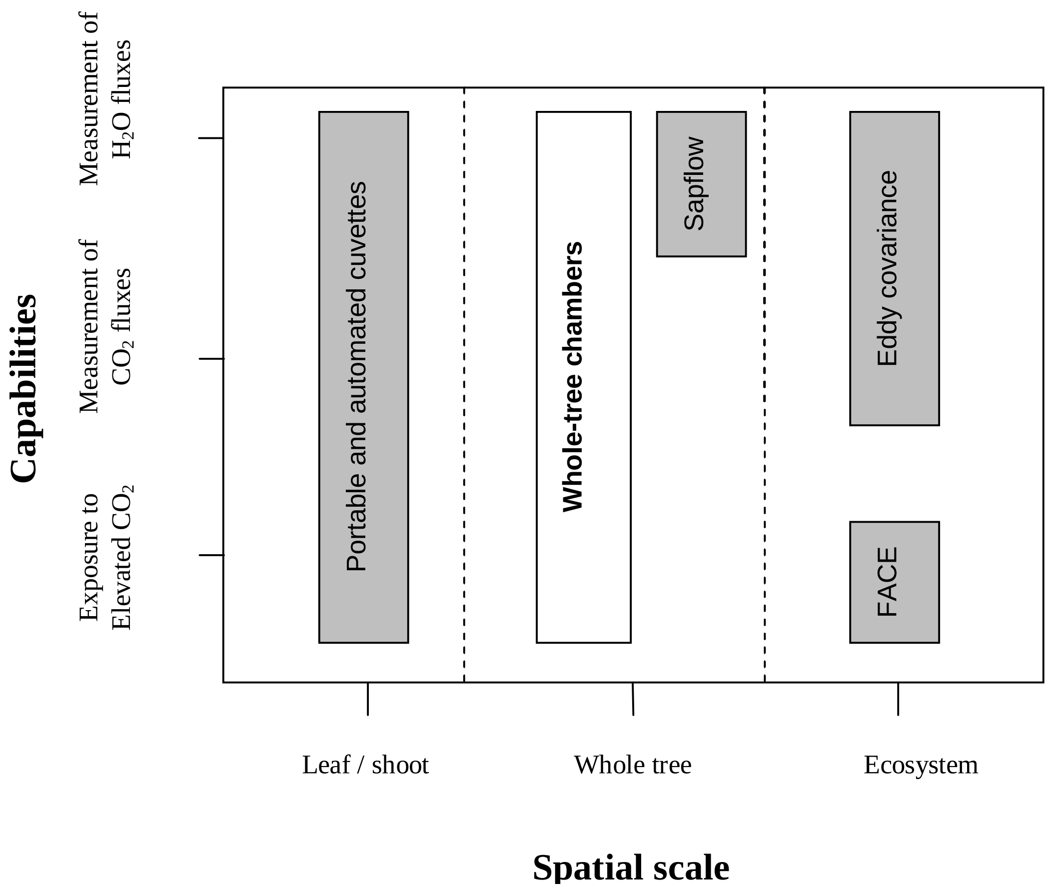
Capabilities
Measurement of H_2O fluxes
Measurement of CO_2 fluxes
Exposure to Elevated CO_2
Portable and automated cuvettes
Whole-tree chambers
Sapflow
Eddy covariance
FACE
Leaf / shoot
Whole tree
Ecosystem
Spatial scale

Fig. 9.